

**Regular Article****Chemical Activation of Piezo1 Alters Biomechanical Behaviors toward Relaxation of Cultured Airway Smooth Muscle Cells**Mingzhi Luo,\*<sup>#</sup> Kai Ni,<sup>#</sup> Rong Gu, Youyuan Qin, Jia Guo, Bo Che, Yan Pan, Jingjing Li, Lei Liu, and Linhong Deng\**Changzhou Key Laboratory of Respiratory Medical Engineering, Institute of Biomedical Engineering and Health Sciences, Changzhou University, Changzhou, Jiangsu 213164, China.*

Received March 28, 2022; accepted September 12, 2022

Inspired by the well-known phenomenon of stretch-induced airway dilation in normal lungs and the emerging stretch-responsive Piezo1 channels that can be chemically activated by specific agonists such as Yoda1, we attempted to investigate whether chemical activation of Piezo1 by Yoda1 can modulate the biomechanical behaviors of airway smooth muscle cells (ASMCs) so that it may be exploited as a novel approach for bronchodilation. Thus, we treated *in vitro* cultured rat ASMCs with Yoda1, and examined the cells for calcium signaling, cell stiffness, traction force, cell migration, and the mRNA expression and distribution of molecules relevant to cell biomechanics. The data show that ASMCs expressed abundant mRNA of Piezo1. ASMCs exposed to 1  $\mu$ M Yoda1 exhibited a potent but transient Ca<sup>2+</sup> signaling, and treatment with 1  $\mu$ M Yoda1 for 24 h led to decreased cell stiffness and traction force, all of which were partially reversed by Piezo1 inhibitor GsMTx4 and Piezo1 knockdown, respectively. In addition, ASMCs treated with 1  $\mu$ M Yoda1 for 24 h exhibited impaired horizontal but enhanced vertical cell migration, as well as significant changes in key components of cells' contractile machinery including the structure and distribution of stress fibers and alpha-smooth muscle actin ( $\alpha$ -SMA) fibrils, the mRNA expression of molecules associated with cell biomechanics. These results provide the first evidence that chemical activation of Piezo1 by Yoda1 resulted in marked pro-relaxation alterations of biomechanical behaviors and contractile machinery of the ASMCs. These findings suggest that Piezo1-specific agonists may indeed have great potential as alternative drug agents for relaxing ASMCs.

**Key words** airway hyperresponsiveness, airway smooth muscle cell, Piezo1, Yoda1, biomechanical behavior

**INTRODUCTION**

Biomechanical behaviors of airway smooth muscle cells (ASMCs) such as cell stiffness and traction force largely determine the contraction and relaxation of bronchial airways during both physiological and pathological processes such as the airway structural formation in healthy lungs and the excessive airway narrowing due to airway hyperresponsiveness (AHR) in asthma.<sup>1–3</sup> Asthma is a chronic respiratory disease characterized by airway remodeling, airway inflammation, and AHR, all of which involve aberrant behaviors of ASMCs.<sup>4–8</sup> Particularly, ASMCs are considered the end-effector of AHR because AHR is actually instigated by the hypercontraction of ASMCs, which abnormally decreases airway diameter and thereby leads to airflow obstruction.<sup>9–12</sup> Therefore, it is critically important to dilate the constricted airways *via* relaxation of ASMCs in asthma therapy. Currently,  $\beta_2$ -adrenoceptor ( $\beta_2$ AR) agonists such as salbutamol are commonly prescribed for bronchodilation since they can potently relax ASMCs. These bronchodilators are effective for the majority of asthma patients, especially those with mild and moderate symptoms, but not effective for a considerable population of severe asthma patients whose symptoms remain poorly controlled.<sup>4,13–16</sup> In addition, long-term administration of  $\beta_2$ -AR-agonists decreases  $\beta_2$ -AR expression and leads to insensitivity and desensitization of these  $\beta_2$ -AR-agonists, which has been

associated with tachyphylaxis.<sup>17,18</sup> Even more, it has been observed in various clinical trials that chronic treatment with  $\beta_2$ -AR agonists can cause increased bronchial hyper-reactivity and other adverse effects.<sup>19</sup> In order to overcome the limitations of  $\beta_2$ -AR agonists, other pharmacological agents are being explored for their potential as alternative therapeutic drug candidates for bronchodilation. For example, bitter substances that are widely available from natural sources such as naringin have been recently reported to have great potency for relaxing ASMCs *via* activating bitter taste receptors (TAS2R) expressed on the cell membrane, even though they still have various issues to be carefully evaluated such as their potential adverse effect on other components of the airways such as epithelium.<sup>20,21</sup> Taken together, it is obviously highly desirable to develop new therapies functioning independently from  $\beta_2$ -adrenergic pathways.

Interestingly, it is known that ASMCs can be relaxed not only chemically by various chemical agents but also physically by mechanical forces.<sup>22</sup> For example, it has long been reported that *in vitro* application of cyclic stretch can reduce both the active force of a pre-contracted muscle strip and the traction force generated by cultured ASMCs, whereas *in vivo* a deep inspiration can dilate spasmogen-contracted airways.<sup>23–25</sup> Studies suggest that mechanical stretch may relax ASMCs *via* the activation of transmembrane Piezo1 channels.<sup>26</sup> Piezo1 is a novel mechanosensitive molecule and its activation can initiate a series of cellular responses such as proliferation and migration depending on the cell type and

<sup>#</sup>These authors contributed equally to this work.

\* To whom correspondence should be addressed. e-mail: luomingzhi@cczu.edu.cn; dlh@cczu.edu.cn

related microenvironment. Moreover, Piezo1 activation is unlikely to have an adverse effect on the airway components since the airways are always exposed to continuous cyclic stretch during a tidal breath and deep inspiration *in vivo*. It is also worth noting that although Piezo1 primarily responds to physical stretch, it can also be chemically activated by specific agonists such as Yoda1.<sup>27)</sup> Therefore, considering convenience for clinical application, chemical activation of Piezo1 may be advantageous in terms of bronchodilation in asthma therapy.<sup>28)</sup> However, it is so far unclear whether and how chemical activation of Piezo1 by Yoda1 would modulate biomechanical behaviors of ASMCs, which is apparently essential in the development of Piezo1-mediated novel bronchodilators.

To address this question, we treated *in vitro* cultured rat ASMCs mainly with Piezo1 specific agonist Yoda1, since it has a much lower EC<sub>50</sub> than other agonists such as Jedi1 and Jedi2,<sup>29,30)</sup> and then assessed the cells' biomechanical behaviors including cell stiffness, traction force, and migration. We found that treatment with Yoda1 resulted in altered biomechanical behaviors which all suggest relaxation of the ASMCs, together with changes in the mRNA expression and organization of key intracellular molecules responsible for cellular biomechanical behaviors. These findings indicate that chemical activation of Piezo1 indeed alters biomechanical behaviors towards relaxation of ASMCs, which may provide useful insight into further exploration and development of Piezo1 agonists as novel bronchodilators.

## MATERIALS AND METHODS

**Materials** Fluo-4 acetoxymethyl ester (Fluo-4/AM) (#93596), transferrin (#T8158), Jedi1 (#SML2533), and insulin (#91077C) were purchased from Sigma-Aldrich (St. Louis, MO, U.S.A.). GsMTx4 (#ab141871) was purchased from Abcam (Cambridge, MA, U.S.A.). Collagen type I (#08-115) was purchased from Merck. Dulbecco's modified Eagle's medium (#11965-084, DMEM), fetal bovine serum (#16000-044, FBS), penicillin-streptomycin (#15140122), and trypsin (#25200056) were purchased from Thermo Fisher Scientific, Inc. (Waltham, MA, U.S.A.). Cell culture flasks (#3073) and plates (#CLS3506) were purchased from Corning Incorporated (Corning, NY, U.S.A.). Yoda-1 (#HY-18723) was purchased from MedChemExpress (MCE, Shanghai, China). All other reagents were purchased from Fisher Scientific unless noted otherwise.

**Primary Culture of ASMCs and Treatment with Stretch or Yoda1** Primary ASMCs were isolated from Sprague Dawley (SD) rats according to the previously described method which was approved by the Committee of Changzhou University on Studies Ethics.<sup>31,32)</sup> The rats (180–220 g; 6–8 weeks) were purchased from Cavens Lab Animal Co., Ltd. (Changzhou, China) and raised in pathogen-free conditions at approx. 25 °C, provided with a 12 h light–dark cycle and free access to food and water. The use of animals in experiments is regulated under the Institutional Guidelines for Animal Care and Use Committee of Changzhou University (Changzhou, China). Before experiments, the rats were first anesthetized by treating them with an intraperitoneal injection of pentobarbital sodium (60 mg/kg). Then the tracheas were harvested and the connective tissues were detached. After cutting longitudinally, the tracheas were treated with 0.25% trypsin–0.02% ethylenediaminetetraacetic acid (EDTA) in Hanks' balanced salt solu-

tion (in mM: 5 KCl, 0.3 KH<sub>2</sub>PO<sub>4</sub>, 138 NaCl, 4 NaHCO<sub>3</sub>, 0.3 Na<sub>2</sub>HPO<sub>4</sub>, and 1.0 glucose) for 20 min at 37 °C, so that the cells were enzymatically dissociated. Dissociated cells were centrifuged, resuspended in DMEM supplemented with 10% FBS and antibiotics, seeded into culture flasks, and incubated at 37 °C in humidified air containing 5% CO<sub>2</sub>. ASMCs were identified with an anti-alpha-smooth muscle actin ( $\alpha$ -SMA) antibody (#ab119952, Abcam, MA, U.S.A.). These cells showed a typical “hill and valley” appearance under phase-contrast microscopy and physiological response to agonists. The cells at a passage of 3–10 were used for experiments.

For stretch treatment, exponentially proliferating ASMCs ( $4 \times 10^5$  cells/cm<sup>2</sup>) were cultured in 6 well plates for 48 h, and culture media was changed with FBS-free basic DMEM media. ASMCs were then exposed to a high stretch (13% strain, 0.5 Hz, simulating the conditions during deep inspiration) for 48 h by using an FX-5000 device (Flexcell International, Hillsborough, NC, U.S.A.). For Yoda1 treatment, exponentially proliferating ASMCs ( $1-4 \times 10^5$  cells/cm<sup>2</sup>) were cultured for 24 h and culture media was changed with FBS-free basic DMEM media. ASMCs were then exposed to either Yoda1 (1, 5, or 10  $\mu$ M) as experimental groups or dimethyl sulfoxide (DMSO) (0.1%) as vehicle control groups for 24 h.

For experiments involving inhibitors, cells were exposed to the inhibitors for 0.5 h, unless stated otherwise, in the presence or absence of Yoda1. For inhibiting the function of mechanically sensitive ion channels, cells were treated with GsMTx4 (5  $\mu$ M). To remove calcium ions from the DMEM, ethylene glycol tetraacetic acid (EGTA) (2 mM, #E3889; Sigma) was added to the medium.

**Assessment of mRNA Expression of Relevant Genes in ASMCs** The level of mRNA expression of relevant genes in ASMCs was assessed by real-time quantitative PCR (qPCR). The cells were cultured in the 6-well plates until they reached 85 to 90% confluence and the medium was replaced with FBS-free basic DMEM media containing 1  $\mu$ M Yoda1 or DMSO (0.1%) for 24 h. Total RNA from cultured ASMCs was extracted using the TRI Reagent RNA Isolation Reagent (#T9424, Sigma). Five hundred nanograms total RNA was used to generate 1st strand cDNA using the Revert Aid First Strand cDNA Synthesis Kit (#K1622, Thermo Fisher Scientific, Inc.). The associated primers used were shown in Supplementary Table S1 and purchased from General Biosystems (Anhui, China). PowerUp SYBR Green Master Mix (#A25742, Applied Biosystems, CA, U.S.A.) was used. The reaction was run in the qPCR system (StepOnePlus, Applied Biosystems) using 1  $\mu$ L of the cDNA in a 10  $\mu$ L reaction according to the manufacturer's instructions in triplicate. Calibration and normalization were done using the 2<sup>− $\Delta\Delta$ CT</sup> method, where  $\Delta$ CT = C<sub>T</sub> (target gene) – C<sub>T</sub> (reference gene) and  $\Delta\Delta$ CT = C<sub>T</sub> (1  $\mu$ M Yoda1 groups) – C<sub>T</sub> (0.1% DMSO groups). Fold changes in mRNA expression of different genes were calculated as the ratio of experiment groups to the control groups from the resulting 2<sup>− $\Delta\Delta$ CT</sup> values from three independent experiments.

To silence the expression of Piezo1 in rat ASMCs, Negative Control Medium GC Duplex #2 (Thermo Fisher Scientific, Inc.) and small interfering RNA (siRNA) interference for rat Piezo1 (#S0829, Ribo Biotechnology CO., Guangdong, China) were used. Briefly, cells were seeded in 6-well plates at  $1 \times 10^6$  cells/well for 24 h before transfection. At 90% confluence, the cells were transfected with 30 nmol/L siRNA using

Lipofectamine RNAi MAX (#13778, Invitrogen) in OptiMEM according to the manufacturer's instructions. Transfection mixes were applied to the cells for 24h, and subsequently were removed and replaced with 2mL of growth media. The cells were cultured for 48h before use in experiments. The mRNA expression levels of Piezo1 were ascertained by qPCR.

**Assessment of Intracellular  $[Ca^{2+}]_i$  in ASMCs** The dynamic response of  $[Ca^{2+}]_i$  in ASMCs was visualized using Fluo-4/AM as described previously.<sup>33)</sup> Briefly, cultured ASMCs were seeded into confocal Petri dishes ( $1 \times 10^5$  cells per dish) and cultured for 24h, after which the cells were incubated with  $5 \mu\text{M}$  Fluo-4/AM for 30 min at  $37^\circ\text{C}$ . Then the cells were incubated for 20 min in Tyrode solution to allow de-esterification of Fluo-4/AM. The fluorescence images were recorded by a laser scanning confocal microscope (LSM710, Carl Zeiss, Jena, Germany) at 488 nm/505 nm for the excitation/emission wavelengths. The cells were first measured for 20s to achieve baseline fluorescence over entire cells ( $F_0$ ). Then Yodal was added to the cells and the cells were continuously measured for 200s ( $F$ ). Subsequent image processing and analysis were performed by using Image J software (NIH, Bethesda, MD, U.S.A.).  $[Ca^{2+}]_i$  was represented as  $F/F_0$ .

**Assessment of Cell Viability and Proliferation of ASMCs** The cell viability was assessed by the procedure of the Cell Counting Kit-8 (CCK-8) assay kit (#C0037, Beyotime Biotechnology, Shanghai, China). Cells were plated in 96-well plates at a density of  $1 \times 10^4$  cells/well. After overnight cultivation, the cells were bathed in serum-free culture media containing  $1 \mu\text{M}$  Yodal or vehicle (0.1% DMSO) for 24h, and the  $10 \mu\text{L}$  of CCK-8 solution was added to the cells for 1h at  $37^\circ\text{C}$ . Absorbance was acquired by using an automatic microplate reader at 450 nm (Elx100, Thermo Fisher Scientific, Inc.).

The cell proliferation was assessed by using the trypan blue exclusion cell counting method. To this end, ASMCs were seeded at the density of  $2 \times 10^4$  cells/cm<sup>2</sup> into 6-well plates for 24h. Then the medium was replaced with fresh serum-free basal media containing Yodal at different concentrations. After the cells were incubated for 24h with/without Yodal, cell number was counted by using a cytometer after staining with 0.4% trypan blue for living cells. The cell proliferation is presented as a ratio of cell number in the experimental group to that in the vehicle group.

**Assessment of Cell Morphology of ASMCs** Cultured ASMCs were treated with different concentrations of Yodal for 24h and then imaged by phase-contrast microscopy using an inverted optical microscope with a  $10 \times$  objective (Primovert, Carl Zeiss). The view-fields for imaging were chosen randomly to prevent subjective bias. The single cell area was evaluated by ImageJ software. Fold change in cell area was calculated as a ratio of the cell area in the experimental groups to that in the control groups in three independent experiments ( $N > 100$  cells).

**Assessment of Cell Stiffness of ASMCs** Cell stiffness of cultured ASMCs was measured by optical magnetic twisting cytometry (OMTC) as described previously.<sup>33)</sup> In brief, ASMCs cultured on type I collagen-coated dishes (96-well plate, Immulon II) were bathed in serum-free culture media containing  $1 \mu\text{M}$  Yodal or vehicle (0.1% DMSO) for 24h. Then the cells were first labeled with Arg-Gly-Asp (RGD)-coated ferrimagnetic microbeads for 20min and washed with DMEM to remove unbound beads. Then the microbeads were

magnetized horizontally with a brief 1000-Gauss pulse and twisted in a vertically aligned homogenous magnetic field (20 Gauss) oscillating at 0.75Hz, resulting in rotation and displacement of the bead. In this study, the cells were also twisted in the oscillatory magnetic field at a frequency consecutively increasing from 0.1 to 100Hz, in order to assess the cell stiffness dependence on the twisting frequency. The cell stiffness ( $G'$ ) was measured as the ratio between the applied magnetic torque and bead displacement (Pa/nm).

**Assessment of Cell Traction Force of ASMCs** Traction force generated by ASMCs was measured by using Fourier transformation traction force microscopy (FTTFM) as described previously.<sup>32,33)</sup> Briefly, ASMCs were cultured in serum-free DMEM containing  $1 \mu\text{M}$  Yodal or vehicle (0.1% DMSO) for 24h and then seeded onto type I collagen (5000 cells/dish)-coated polyacrylamide gel in DMEM without FBS for 6h. A single cell and the fluorescent microbeads (Molecular Probes, Eugene, OR, U.S.A.) were then imaged by phase-contrast and fluorescence microscopy, respectively. Then NaOH was added to cell cultures and the cell-free bead positions were recorded as a reference point (traction-free) for bead displacement. The traction force was calculated from the displacement of microbeads averaged over the cell area before and after the treatment of NaOH.

**Assessment of Cell Migration of ASMCs** Migration of ASMCs was assessed in terms of either horizontal cell migration *via* scratch wound healing or vertical cell migration *via* transwell assay. In wound healing assay of horizontal cell migration, the cells were cultured in 6-well plates (Corning, NY, U.S.A.) until a confluent monolayer was achieved. Experimental scratch wound was made across the cell monolayer using a sterile micropipette tip, then the cells were washed 3 times with sterile phosphate buffered saline (PBS). The cells were bathed in starvation culture media containing  $1 \mu\text{M}$  Yodal. As a control, cells were bathed in a maximal concentration of vehicle (0.1% DMSO). Wound areas were observed and recorded at 0, 4, 8, 12, and 24h by using a Cell Observer System (Carl Zeiss) equipped with a CO<sub>2</sub> and temperature control chamber. The experimental wound area was quantified manually using "Area measurement" in ImageJ software and normalized to the initial wound area at the start of the experiment, and the migration rate was defined by the ratio of the wound healing area in Yodal treated groups to that of controls. ImageJ software and Matlab (The MathWorks) were used to analyze the migration rate of single ASMC.

In transwell assay of vertical cell migration, cells in serum-free medium ( $1 \times 10^5$  cells/well) were placed in the upper chamber of transwell culture dish (#07-200-169, Corning), which was separated by a filter membrane with  $8 \mu\text{m}$  pores from the lower chamber filled with 2mL complete medium. Cells were allowed to settle for 6h before  $1 \mu\text{M}$  Yodal was added to the upper chamber. As a control, maximal concentration of vehicle (0.1% DMSO) was added in the upper chamber instead of Yodal. 24h later, cells were fixed with 4% paraformaldehyde (#30525-89-4, Electron Microscopy Sciences, Hatfield, PA, U.S.A.). The non-migrated cells that remained in the upper chamber were removed with cotton swabs, and the cells vertically migrated through the membrane pores into the lower chamber were stained with 0.1% crystal violet (#C6158; Sigma) for 10min at room temperature (r.t.), before being examined and imaged by light microscopy at 10X magnification

(Olympus BX60; Olympus Corporation, Tokyo, Japan). Then the number of stained cells was counted by using ImageJ software. Results were based on the analysis of 10 randomly selected fields per transwell in each condition and each experiment was repeated three times.

**Assessment of Stress Fiber and Alpha-Smooth Muscle Actin in ASMCs** The distribution of stress fiber and  $\alpha$ -SMA was assessed by immunofluorescent staining. In brief, cells were fixed in 3.7% paraformaldehyde for 15 min at r.t., then permeabilized with 0.5% Tween-X-100 for 15 min at r.t. Non-specific binding of the antibodies was blocked by incubating the samples in PBS containing 1% bovine serum albumin (BSA) for 1 h at r.t. The stress fiber or F-actin (red) was stained with a fluorescent red phalloidin and nuclei (blue) were stained with 4'-6-diamidino-2-phenylindole (DAPI) for 10 min at r.t. in the dark. The  $\alpha$ -SMA was stained by incubating the cells first with  $\alpha$ -SMA monoclonal antibody (#MA5-11547, Thermo Fisher Scientific, Inc.) for 24 h at 4°C, then with fluorescently labeled secondary antibodies (goat anti-rabbit conjugated to fluorescein isothiocyanate (FITC), #F-2761, Thermo Fisher Scientific, Inc.) for 1 h at r.t. in the dark. Between all staining steps, cells were washed 3 times with PBS. Stained cells were visualized with laser scanning confocal microscopy (LSM710, Carl Zeiss) using oil objective (63 $\times$ ). Acquisition parameters were kept constant during the experiments. Fluorescent images were processed with ImageJ software.

**Statistical Analysis** Statistical analysis was performed by using GraphPad Prism 8.0 (Graph Pad Software, San Diego, CA, U.S.A.). Data were analyzed with a Shapiro–Wilk normality test using Origin 2018 (OriginLab Corporation, Northampton, MA, U.S.A.). OMTC original data followed LogNormal distribution and thus were transformed by taking the natural log of all original data before analysis. Other data followed Normal distribution. Therefore, data were reported as means  $\pm$  standard error of the mean (S.E.M.), and group size ( $n$ ) represents the number of experiments. Comparisons of means between two groups were performed by unpaired Student's  $t$ -test. Comparisons of means among three or more groups were performed by One-way or Two-way ANOVA followed by Tukey's *post hoc* test (Tukey HSD method). The significance of the mean comparisons is represented by asterisks (\* $p$  < 0.05; \*\* $p$  < 0.01).

## RESULTS

**Yodal Activated Piezo1 Expressed in ASMCs** Since ASMCs *in vivo* are known to express Piezo1 which is involved in airway responses to continuous stretch during tidal breathing and deep inspiration, we first ascertained the mRNA expression of Piezo1 in ASMCs cultured in conditions with/out stretch (13% strain to mimic DI). As shown in Supplementary Fig. S1A, mRNA expression of Piezo1 in the cells cultured without stretch (static conditions) was 54% as normalized to the expression of glyceraldehyde-3-phosphate dehydrogenase (GAPDH) (acting as an internal reference), indicating an abundant expression of Piezo1 in the cultured ASMCs. In comparison, mRNA expression of Piezo1 in the cells cultured with the stretch condition for 48 h was 34%, decreasing by about 40% when compared to that in the static groups ( $p$  < 0.01).

It has been reported that contractile and proliferative smooth muscles may have different Piezo1 expressions.<sup>34)</sup> In

this study, we mainly used cultured proliferative ASMCs. To test whether contractile ASMCs *in vivo* also express Piezo1, we compared the Piezo1 mRNA expression in freshly isolated ASMCs (P0, contractile phenotype), and cultured cells (proliferative phenotype) in the passage of 5 (P5) and P10. As shown in Supplementary Fig. S1B, the freshly isolated ASMCs had more Piezo1 mRNA than the cultured ASMCs of P5 and P10, but the latter two had similar levels of Piezo1 mRNA expression. These data indicate that both *in vitro* and *in vivo* rat ASMCs indeed expressed abundant Piezo1 which may respond to mechanical and chemical activation.

We then evaluated, with 3-(4,5-dimethylthiazol-2-yl)-2,5-diphenyltetrazolium bromide (MTT), CCK-8 assays, and cell counting, the impact of Yodal treatment at concentrations of 1, 5, and 10  $\mu$ M, respectively on the cellular activity and proliferation of ASMCs, in order to screen a safe dosage of Yodal treatment for the following experiments. As shown in Fig. 1A, the MTT assay demonstrated that Yodal treatment for 24 h at 5 and 10  $\mu$ M dramatically decreased cellular activity of ASMCs, whereas no impact on cellular activity at 1  $\mu$ M. CCK-8 assay and cell counting results showed a similar effect of Yodal treatment on cellular activity and cell proliferation, respectively (Figs. 1B, C). To further confirm this phenomenon, morphology of ASMCs was observed under a light microscope, and the results showed that ASMCs treated with 1  $\mu$ M Yodal became thin and had more protrusions, but most of ASMCs treated with 5 and 10  $\mu$ M Yodal became round or were broken (Supplementary Fig. S2A), while Yodal treatment consistently decreased cell area (Supplementary Fig. S2B). These results suggest that 1  $\mu$ M is a safe dosage for Yodal treatment of ASMCs and was thus used for all the following experiments.

Subsequently, we evaluated whether Yodal could chemically activate Piezo1, by characterizing  $[Ca^{2+}]_i$  dynamics in ASMCs after treatment with 1  $\mu$ M Yodal or vehicle (1% DMSO). The result indicated that  $[Ca^{2+}]_i$  transiently increased in ASMCs after treatment with 1  $\mu$ M Yodal (Fig. 1D). It is known that Yodal-induced calcium signaling is mainly mediated by calcium influx through Piezo1.<sup>29,30)</sup> To confirm this, we treated ASMCs with 2 mM ethylene glycol tetraacetic acid (EGTA) for 15 min to deplete extracellular calcium content before application of Yodal, which significantly decreased Yodal-induced calcium signaling, suggesting the signaling was mainly due to influx of extracellular calcium. To test whether the Yodal-enhanced calcium signaling was mediated specifically through Piezo1, we pretreated the ASMCs with GsMTx4 (Piezo1 inhibitor), followed by exposure to Yodal. As shown in Fig. 1D, pretreatment with GsMTx4 significantly abrogated the Yodal-enhanced calcium signaling.

To further confirm the specificity of Piezo1 in mediating Yodal-enhanced calcium signaling, we silenced the mRNA expression of Piezo1 in ASMCs by using siRNA. qPCR results confirmed that the efficiency of Piezo1 knockdown (KD) was approx. 80% (Supplementary Fig. S1C). When ASMCs with Piezo1 KD were exposed to 1  $\mu$ M Yodal, the cells responded with decreased calcium signaling (Fig. 1E). These results together confirmed that Yodal induced chemical activation of Piezo1, which initiated a transient calcium signaling *via*  $Ca^{2+}$  influx.

To compare the effect of Yodal-induced chemical activation of Piezo1 with stretch-induced mechanical activation of

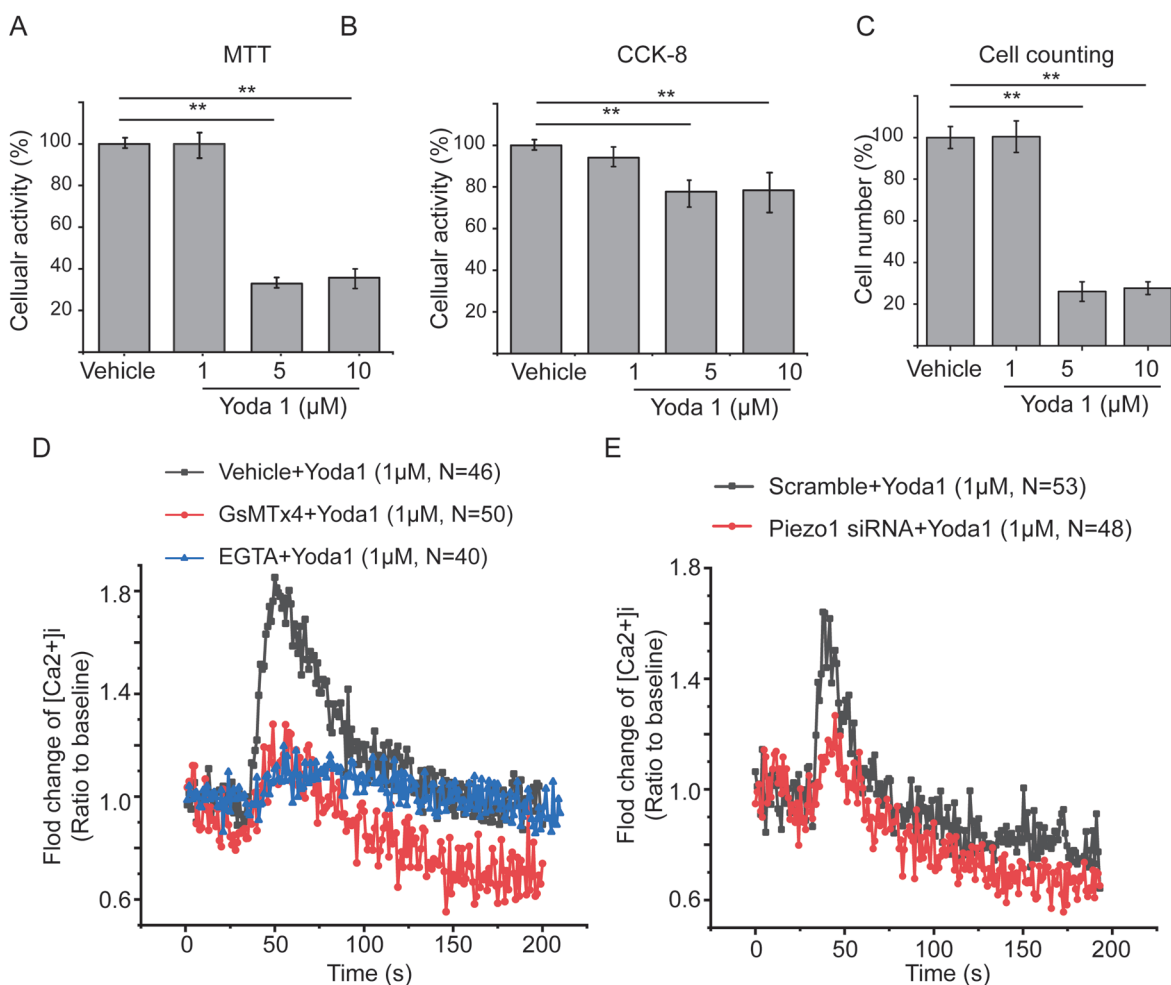


Fig. 1. Yodal Activated Piezo1 Expressed in ASMCs

(A–C) MTT, CCK-8 assay, and cell counting results of cellular activity and proliferation of ASMCs treated with or without Yodal, respectively. The dose of Yodal was 1, 5, and 10 μM, respectively, and the vehicle was 1% DMSO in DMEM. Data were shown as means ± S.E.M. ( $n = 3$  experiments). \*\* $p < 0.01$ . Comparisons were made using One-way ANOVA followed by Tukey's *post hoc* test. (D, E) Time-courses of changing relative mean fluorescence intensity of Fluo-4 in cultured ASMCs pretreated with or without EGTA, GsMTx4, and Piezo1 KD in response to 1 μM Yodal. Each experiment assayed 40–60 cells and was repeated three times.

Piezo1, we also detected the mRNA expression of Piezo1 in ASMCs after treated with 1 μM Yodal or vehicle (1% DMSO). Interestingly, 1 μM Yodal induced approx. 50% reduction in the mRNA expression of Piezo1 from the baseline level with vehicle (1% DMSO) (Supplementary Fig. S1D), which is comparable to that 13% stretch-induced approx. 40% reduction in mRNA expression of Piezo1 from the baseline level in static condition (Supplementary Fig. S1A). These results suggest that chemical activation of Yodal may initiate a similar effect of mechanical stretch.

**Yodal Decreased Stiffness and Traction Force of ASMCs via Piezo1 Activation** Stretch conditions during deep inspiration have been reported to relax ASMCs.<sup>23–25</sup> To test whether Yodal-induced chemical activation could lead to the relaxation of ASMCs as the effect of deep inspiration, we evaluated the impact of Yodal treatment on stiffness and traction force (major determinants of cell relaxation) of ASMCs using OMTC and FTTFM, respectively. As shown in Fig. 2A, the stiffness of ASMCs increased in a frequency-dependent manner whether the cells were treated with Yodal or vehicle. However, the stiffness of Yodal-treated ASMCs was significantly decreased from the vehicle-treated cells (Fig. 2A,  $p < 0.01$ ). Apart from cell stiffness, the traction

force of Yodal-treated ASMCs was also dramatically decreased from their vehicle-treated counterparts (from 250 to 160 Pa,  $p < 0.01$ ), as shown in Fig. 2B. Another Piezo1 specific agonist, Jedi1 (50 μM) caused similar effects on cell stiffness, traction force, and transient calcium signaling of cultured ASMCs (Supplementary Fig. S3A–C).

When ASMCs were cultured in the presence of Piezo1 inhibitor (GsMTx4) or Piezo1 knockdown (Piezo1 siRNA) the reduction of cell stiffness and traction force in response to 1 μM Yodal were significantly attenuated, although GsMTx4 and Piezo1 siRNA did not seem to completely inhibit the reduction of cell stiffness and traction force due to Yodal (Yodal vs. Yodal + GsMTx4, Yodal vs. Yodal + Piezo1 siRNA, \*\* $< 0.01$ , Figs. 2C, D, respectively). We speculate that GsMTx4 or Piezo1 siRNA may only partially inhibit the function of Piezo1. These data together indicate that chemical activation of Piezo1 did decrease cell stiffness and traction force simultaneously *via* activation of Piezo1, which in turn could contribute to the relaxation of ASMCs.

**Yodal Inhibited Horizontal but Enhanced Vertical Migration of ASMCs** Migration is another mechanical behavior of ASMCs, which is essential for airway developing and remodeling. We thus assessed the effect of Yodal treatment on

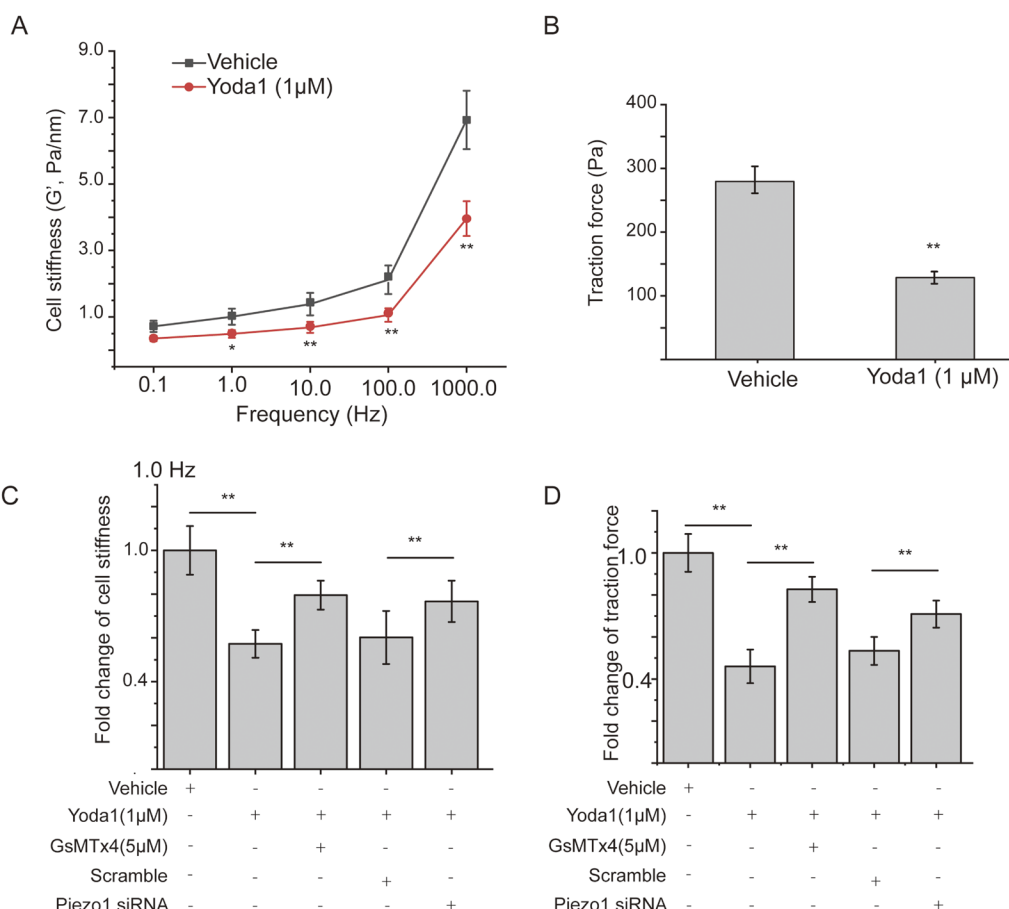


Fig. 2. Chemical Activation of Piezo1 by Yoda1 Decreased Cell Stiffness and Traction Force

(A) Cell stiffness of ASMCs treated with or without 1  $\mu$ M Yoda1 for 24h was measured with optical magnetic twisting cytometry (OMTC) at 0.1, 1.0, 10.0, 100.0, and 1000.0Hz. (B) Traction force of ASMCs treated with or without 1  $\mu$ M Yoda1 for 24h was measured with Fourier transformation traction force microscopy (FTTFM). (C, D) Cell stiffness and traction force of cultured ASMCs pretreated with GsMTx4 and Piezo1 KD followed by 24h treatment of 1  $\mu$ M Yoda1. Data were shown as means  $\pm$  S.E.M. ( $n = 3$  experiments). \* $p < 0.05$ , \*\* $p < 0.01$ . Comparisons were made using Two-way ANOVA followed by Tukey's *post hoc* test (A), unpaired Student's *t*-test (B), and One-way ANOVA followed by Tukey's *post hoc* test (C, D).

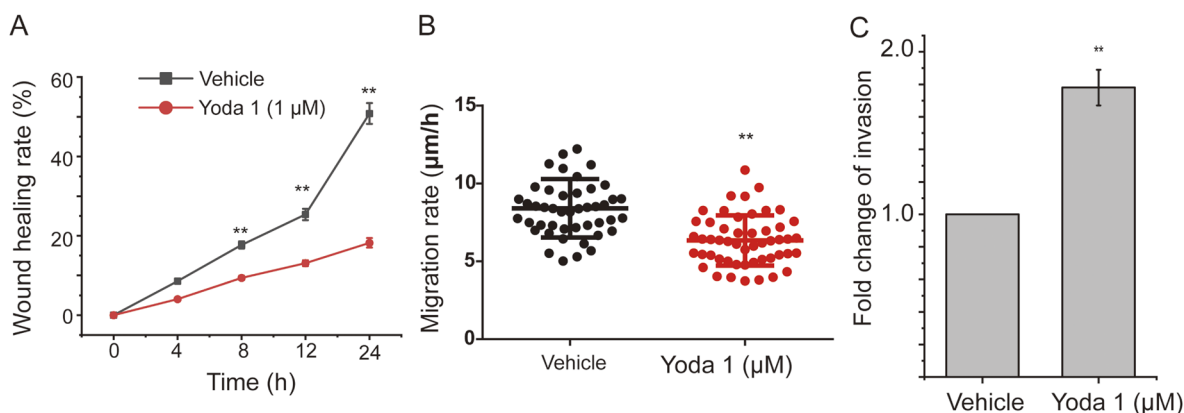


Fig. 3. Chemical Activation of Piezo1 by Yoda1 Inhibited Horizontal but Promoted Vertical Cell Migration of ASMCs

(A) Quantification of wound healing rate and (B) migration rate of ASMCs cultured with or without 1  $\mu$ M Yoda1. (C) Quantification of the fold change of cell number of ASMCs through 8  $\mu$ m pores cultured with or without 1  $\mu$ M Yoda1. Data were shown as means  $\pm$  S.E.M. ( $n = 3$  experiments). \*\* $p < 0.01$ . Comparisons were made using Two-way ANOVA followed by Tukey's *post hoc* test (A) and unpaired Student's *t*-test (B, C).

migration of ASMCs in either horizontal or vertical direction by using wound healing assay or transwell assay, respectively. As shown in Supplementary Fig. S4A of the representative cell migration images during wound healing assay, ASMCs treated with either vehicle or Yoda1 all migrated from the cell-populated area towards the initially cell-free area over 24h,

but the Yoda1-treated cells appeared to migrate much less efficiently. Figure 3A shows the quantified wound healing rate of ASMCs treated by either Yoda1 or vehicle, which clearly demonstrates that the wound healing rate of Yoda1-treated ASMCs was indifferent to that of the vehicle-treated ASMCs in the early stage of wound healing, but became significantly

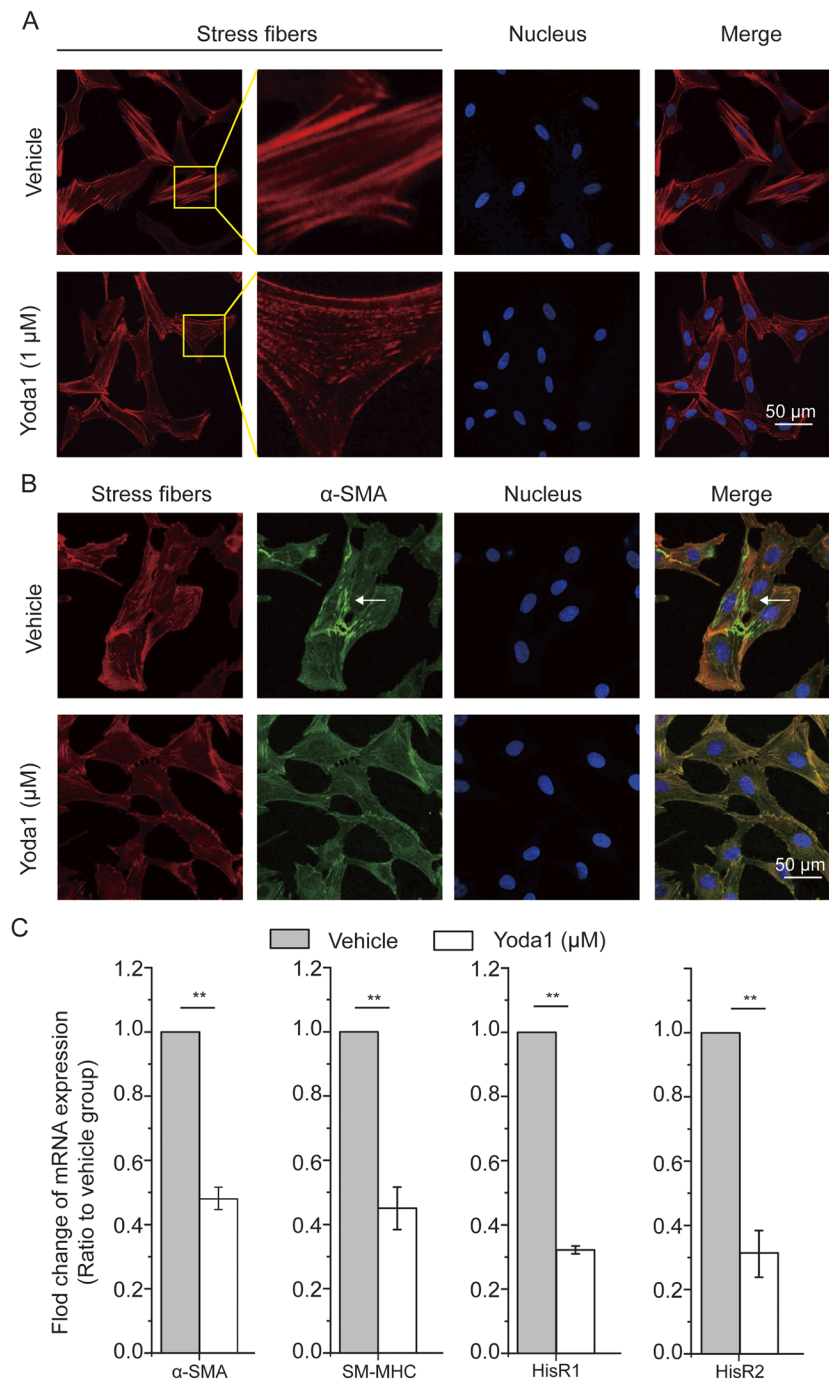


Fig. 4. Chemical Activation of Piezo1 by Yoda1 Disrupted Stress Fibers and Impacted the mRNA Expression of Biomechanical Molecules in AMSCs

(A) Representative immunofluorescence images show the distribution of stress fibers (Red) and nucleus (Blue) in AMSCs treated with or without 1 μM Yoda1. The magnified view of boxed regions was shown in right. Bar = 50 μm. (B) Representative immunofluorescence images show the distribution of stress fibers (Red), α-SMA (Green), and nucleus (Blue) in AMSCs treated with or without 1 μM Yoda1. White arrow shows the distributed α-SMA fibrils alone. Bar = 50 μm. (C) mRNA expression of biomechanical molecules including α-SMA, SM-MHC, and HisR1&2 in AMSCs treated with or without 1 μM Yoda1 was detected by real-time quantitative PCR (qPCR). Data were shown as means ± S.E.M. ( $n = 3$  experiments). \* $p < 0.05$ , \*\* $p < 0.01$ . Comparisons were made using unpaired Student's  $t$ -test (C).

slower than that of the vehicle-treated cells over 8–24h of wound healing ( $p < 0.01$ ). In addition to cell monolayer wound healing assay as shown above, we also quantified the migration rate of individually separated single AMSCs treated with either Yoda1 or vehicle. As shown in Fig. 3B, the migration rate of Yoda1-treated single AMSCs significantly decreased from  $8.04 \pm 1.08$  to  $6.16 \pm 1.38 \mu\text{m}/\text{h}$  when compared to that of the vehicle-treated cells ( $p < 0.01$ ).

Apart from horizontal cell migration, vertical cell migration is also pivotal for airway development and remodeling.

We then assessed the vertical migration capability of AMSCs treated with Yoda1 or vehicle as the cells were cultured in transwell chambers separated by membranes with 8 μm pores. As shown in Supplementary Fig. S4B of the representative images of transwell assay, more Yoda1-treated AMSCs appeared to have migrated from the upper chamber to the lower chamber through the pores in the separating membrane, as compared to their vehicle-treated counterparts. Figure 3C shows the quantified result of the number of cells that eventually passed through the membrane pores (invasion number), which

indicates that the invasion number of Yodal-treated ASMCS was approx. 1.8 fold greater than that of the vehicle-treated cells. Altogether, we clearly show that Yodal-induced chemical activation of Piezol decreased the horizontal but promoted the vertical migration of ASMCS.

**Yodal Induced Changes in the Contractile Machinery of ASMCS** Since the contractile machinery of ASMCS which includes but is not limited to the stress fibers, the contractile proteins and receptors ultimately determine the mechanical behaviors of the cells, we thus evaluated the influence of Yodal on the machinery's some key components as described below. First, we observed the distribution of stress fibers in ASMCS as shown in Fig. 4A. The data show that in vehicle-treated ASMCS the stress fibers were clear and abundant, but in Yodal-treated ASMCS the stress fibers were displayed as dotted fiber structures in much less intensity, suggesting disruption of stress fibers in ASMCS due to Yodal treatment.

We then used immunofluorescence imaging to observe the distribution of  $\alpha$ -SMA in ASMCS treated by either Yodal or vehicle. As shown in Fig. 4B,  $\alpha$ -SMA in the vehicle-treated ASMCS appeared to be not only colocalized with stress fibers, but also formed its own fibril structures (see white arrow). However, in the Yodal-treated ASMCS, no such fibril structures formed by  $\alpha$ -SMA alone were observed. These data indicate that Yodal impacted the intracellular distribution of  $\alpha$ -SMA.

Furthermore, we detected the mRNA expression of contractile proteins including  $\alpha$ -SMA and smooth muscle myosin heavy chain (SM-MHC) as well as histamine receptors in ASMCS treated with either Yodal or vehicle. As shown in Fig. 4C, in Yodal-treated ASMCS the mRNA expression of  $\alpha$ -SMA and SM-MHC significantly decreased as compared to the vehicle-treated cells (by approx. 50% and approx. 45%, respectively,  $p < 0.01$ ). These data indicate that Yodal decreased mRNA expression of  $\alpha$ -SMA and SM-MHC.

Histamine receptors (HisR) are known to mediate the cellular contractile response of ASMCS to histamine during AHR. As shown in Fig. 4C, in Yodal-treated ASMCS the mRNA expression of HisR1 and HisR2 significantly decreased by approx. 70% when compared to the vehicle-treated cells ( $p < 0.01$ ). These data indicate that Yodal reduced the expression of histamine receptors, which may lead to a lowered contractile response of ASMCS to histamine stimulation.

## DISCUSSION

In this study, we found that chemical activation of Piezol by Yodal dramatically decreased cell stiffness and traction force, disrupted the structure and distribution of stress fibers and  $\alpha$ -SMA, and regulated the mRNA expression of molecules associated with cell biomechanics including  $\alpha$ -SMA, SM-MHC, and HisR1&2. These findings revealed a novel regulatory mechanism for relaxing ASMCS by chemically targeting mechanosensitive Piezol channels using specific agonists, which may contribute to development of relevant novel bronchodilators.

In airway walls, ASMCS are continually exposed to mechanical stimulation such as stretch.<sup>35)</sup> A large stretch during deep inspiration is known to modulate biomechanical behaviors of ASMCS, which contributes to multiple processes during physiopathological processes such as bronchodilation

induced in healthy and asthmatics, respectively. Specifically, in healthy subjects the stretch due to deep inspiration causes a beneficial effect on relaxation of ASMCS, but in asthmatics such stretch causes either no effect or sometimes adverse effect on relaxation of ASMCS.<sup>36)</sup> Several mechanosensing receptors such as the TRP family, Piezol&2, and OSCA/TMEM63 have been identified or proposed as mechanically activated ion channels in various mammalian cell types.<sup>37)</sup> These receptors may be mechanically activated and involved in the regulation of biomechanical behaviors of ASMCS. Among them, Piezol is thought to be one of the most promising receptors for mechanosensing, which is characterized by rapid activation in response to stretch.<sup>38)</sup> In this study, by using qPCR, we found that ASMCS express a high level of Piezol mRNA relative to the intracellular level of GAPDH. Importantly, Yodal, a Piezol specific agonist triggered a transient increase of  $Ca^{2+}$  signaling in ASMCS, just as what occurs to the cells in response to physical stretch.<sup>37)</sup> In addition, our data show that Yodal and stretch caused a similar extent of reduction in mRNA expression of Piezol in ASMCS. These results suggest that in alternative to stretch-induced physical activation, Yodal-induced chemical activation of Piezol may also generate mechanically relevant downstream signaling and biological functions in ASMCS.

Biomechanical behaviors such as cell stiffness and traction force are the main determinants of cellular functions for contraction and relaxation. Therefore, measurement of cell stiffness and traction force of ASMCS is not only essential for understanding the pathogenesis of AHR, but also beneficial to finding novel therapeutic targets and strategies for asthma.<sup>39,40)</sup> In this study, activation of Piezol by Yodal decreased cell stiffness and traction force, together with disruption of stress fibers, which is similar to the stretch-induced pro-relaxation effects on ASMCS.<sup>25,41)</sup> However, it is still unknown how elevated  $Ca^{2+}$  signaling following the activation of Piezol triggers the relaxation of ASMCS, although  $Ca^{2+}$  signaling is often considered to initiate excitation-contraction coupling in muscle cells, including ASMCS.<sup>42)</sup> But it has also been reported that  $Ca^{2+}$  signaling can relax artery smooth muscle and ASMCS by activation of BK channels.<sup>43,44,45)</sup> In ASMCS,  $Ca^{2+}$  signaling induced by the activation of bitter taste receptors opens BK channels and thus induces membrane hyperpolarization and the relaxation of ASMCS.<sup>21)</sup> Besides the opening of BK channels, the inhibition of voltage-dependent L-type  $Ca^{2+}$  channels and non-selective cation channels have also been suggested to be involved in TAS2Rs-triggered relaxation of ASMCS.<sup>46,47)</sup> Their roles in Yodal-mediated relaxation of ASMCS may also need to be carefully explored in future.

Another determinant of airway pathological remodeling in asthma is enhanced cell migration of ASMCS.<sup>22,48)</sup> Interestingly, cell migration has also been reported to be modulated by the activation of Piezol.<sup>49)</sup> For example, Han *et al.*<sup>50)</sup> found that Piezol downregulation in prostate cancer cells inhibits its cell migration *in vitro*. Holt *et al.*<sup>4)</sup> found that chemical activation of Piezol by Yodal impairs wound closure in keratinocytes due to increased retraction events. In this study, we found that Yodal-induced chemical activation of Piezol also led to a reduced wound healing rate of *in vitro* cultured ASMCS, which is consistent with the data of a similar experiment with transformed fibroblasts.<sup>51)</sup> The inhibitory effect of Yodal on horizontal cell migration may be partly explained by

the observed inhibitory effects of Yodal on cell traction force and disruption of stress fibers since horizontal cell migration is mainly mediated by cell traction achieved through integrin binding to surrounding extracellular matrix for motility.<sup>52,53)</sup>

On the other hand, we found in transwell assay that Yodal enhanced the vertical cell migration of ASMCs through microscale pores without matrix gel. Such promoting effect of Yodal on vertical cell migration of ASMCs may be partly explained by the observed Yodal-induced decrease of cell stiffness, since decreased cell stiffness may enhance the cell deformability that is required for the cell to easily pass through the microscale pore. In fact, cells are known to migrate in two different modes, one is mesenchymal-like, which depends on integrins and cell traction force, and the other is amoeboid-like, which depends on cell deformation but not integrins. Generally, the integrin-dependent mesenchymal-like cell migration is suitable for 2D surfaces and the integrin-independent amoeboid-like cell migration is suitable for 3D confinement in which cell motility relies on the protrusive flow of actin.<sup>54)</sup> It is also possible that Yodal treatment may cause the ASMCs to switch between the two modes of cell migration, which however needs to be explored in further studies.<sup>52,53)</sup>

In this study, we found that Yodal dramatically inhibited horizontal cell migration of ASMCs at the dose of 1  $\mu$ M. But Mousawi *et al.* reported that Yodal enhanced horizontal cell migration of mesenchymal stem cells at the dose of 0.1–1  $\mu$ M.<sup>55)</sup> In addition, some studies in various cell lines have reported that mRNA expression downregulation or functional inhibition of Piezol can inhibit cell migration and proliferation.<sup>50,56)</sup> These data suggest that the effect of Piezol activation on cell functions may vary depending on the dosage and cell type.

It is worthy to note that this study is limited to *in vitro* cultured rat ASMCs. Therefore, these results need to be further verified in human ASMCs. In addition, this study is limited in the scope and depth of investigation regarding the underlying molecular mechanisms which mediate the changes in cell biomechanics (*e.g.*, cell stiffness and traction force) and the contractile machinery of ASMCs after chemical activation of Piezol. Ultimately, any beneficial effects of chemical activation of Piezol on cell functions of ASMCs related to airway remodeling and AHR need to be fully evaluated in animal models and human subjects of asthma.

Taken together, we demonstrate that chemical activation of Piezol by Yodal alters biomechanical behaviors and the associated contractile machinery which are all conducive to relaxation of ASMCs. These findings provide not only the first evidence that chemically targeting Piezol is as potent as physical stretch in modulation of the biomechanical behaviors of ASMCs, but also useful insight into the potential development of such an approach in bronchodilation.

**Acknowledgments** We thank Mingxing Ouyang (Changzhou University) for the technical support in the horizontal cell migration analysis and Xiang Wang (Changzhou University) for the design of the experiments.

This work was supported by the NSF of China (12072048, 31670950), Key Program of NSF of China (No. 11532003), and the Science and Technology Innovation Leading Plan of High Tech Industry in Hunan Province, China (2020SK2018).

**Author Contributions** ML and LD conceived and designed the experiments. KN, RG, YQ, and JG performed the experiments. KN analyzed the data. BC, JG, YP, JL and LL collected some data for this manuscript. ML and LD revised the manuscript.

All data were generated in-house, and no paper mill was used. All authors agree to be accountable for all aspects of work ensuring integrity and accuracy.

**Conflict of Interest** The authors declare no conflict of interest.

**Supplementary Materials** This article contains supplementary materials.

## REFERENCES

- 1) Jin Y, Liu L, Yu P, Lin F, Shi X, Guo J, Che B, Duan Y, Li J, Pan Y, Luo M, Deng L. Emergent differential organization of airway smooth muscle cells on concave and convex tubular surface. *Front. Mol. Biosci.*, **8**, 717771 (2021).
- 2) Kim HY, Pang M, Varner D, Kojima L, Miller E, Radisky DC, Nelson CM. Localized smooth muscle differentiation is essential for epithelial bifurcation during branching morphogenesis of the mammalian lung. *Dev. Cell*, **34**, 719–726 (2015).
- 3) Bates JH, Maksym GN. Mechanical determinants of airways hyper-responsiveness. *Crit. Rev. Biomed. Eng.*, **39**, 281–296 (2011).
- 4) Holt JR, Zeng W-Z, Evans EL, Woo SH, Ma S, Abuwarda H, Loud M, Patapoutian A, Pathak MM. Spatiotemporal dynamics of Piezol localization controls keratinocyte migration during wound healing. *eLife*, **10**, e65415 (2021).
- 5) West AR, Syong HT, Siddiqui S, Pascoe CD, Murphy TM, Maarsingh H, Deng L, Maksym GN, Bossé Y. Airway contractility and remodeling: links to asthma symptoms. *Pulm. Pharmacol. Ther.*, **26**, 3–12 (2013).
- 6) An SS, Bai TR, Bates JHT, *et al.* Airway smooth muscle dynamics: a common pathway of airway obstruction in asthma. *Eur. Respir. J.*, **29**, 834–860 (2007).
- 7) Chung KF. Should treatments for asthma be aimed at the airway smooth muscle? *Expert Rev. Respir. Med.*, **1**, 209–217 (2007).
- 8) Singapuri A, McKenna S, Brightling CE, Bradding P. Mannitol and amp do not induce bronchoconstriction in eosinophilic bronchitis: further evidence for dissociation between airway inflammation and bronchial hyperresponsiveness. *Respirology*, **15**, 510–515 (2010).
- 9) Chapman DG, Irvin CG. Mechanisms of airway hyper-responsiveness in asthma: the past, present and yet to come. *Clin. Exp. Allergy*, **45**, 706–719 (2015).
- 10) Laudadio RE, Millet EJ, Fabry B, An SS, Butler JP, Fredberg JJ. Rat airway smooth muscle cell during actin modulation: rheology and glassy dynamics. *Am. J. Physiol. Cell Physiol.*, **289**, C1388–C1395 (2005).
- 11) Sakai H, Suto W, Kai Y, Chiba Y. Mechanisms underlying the pathogenesis of hyper-contractility of bronchial smooth muscle in allergic asthma. *J. Smooth Muscle Res.*, **53**, 37–47 (2017).
- 12) Ferguson JE, Patel SS, Lockey RF. Acute asthma, prognosis, and treatment. *J. Allergy Clin. Immunol.*, **139**, 438–447 (2017).
- 13) Siddiqui S, Redhu NS, Ojo OO, Liu B, Irechukwu N, Billington C, Janssen L, Moir LM. Emerging airway smooth muscle targets to treat asthma. *Pulm. Pharmacol. Ther.*, **26**, 132–144 (2013).
- 14) Douros K, Everard ML. Time to say goodbye to bronchiolitis, viral wheeze, reactive airways disease, wheeze bronchitis and all that. *Front. Pediatr.*, **8**, 218 (2020).
- 15) Anthracopoulos MB, Everard ML. Asthma: a loss of post-natal homeostatic control of airways smooth muscle with regression toward a pre-natal state. *Front. Pediatr.*, **8**, 95 (2020).

- 16) Malmstrom K, Rodriguez-Gomez G, Guerra J, Villaran C, Piñeiro A, Wei LX, Seidenberg BC, Reiss TF. Oral montelukast, inhaled beclomethasone, and placebo for chronic asthma. A randomized, controlled trial. *Ann. Intern. Med.*, **130**, 487–495 (1999).
- 17) Olin JT, Wechsler ME. Asthma: pathogenesis and novel drugs for treatment. *BMJ*, **349** (nov24 8), g5517 (2014).
- 18) An SS, Wang WC, Koziol-White CJ, Ahn K, Lee DY, Kurten RC, Panettieri RA Jr, Liggett SB. Tas2r activation promotes airway smooth muscle relaxation despite beta(2)-adrenergic receptor tachyphylaxis. *Am. J. Physiol. Lung Cell. Mol. Physiol.*, **303**, L304–L311 (2012).
- 19) Lin R, Degan S, Theriot BS, Fischer BM, Strachan RT, Liang J, Pierce RA, Sunday ME, Noble PW, Kraft M, Brody AR, Walker JK. Chronic treatment *in vivo* with beta-adrenoceptor agonists induces dysfunction of airway beta(2)-adrenoceptors and exacerbates lung inflammation in mice. *Br. J. Pharmacol.*, **165**, 2365–2377 (2012).
- 20) Ni K, Guo J, Bu B, Pan Y, Li J, Liu L, Luo M, Deng L. Naringin as a plant-derived bitter tastant promotes proliferation of cultured human airway epithelial cells *via* activation of tas2r signaling. *Phytomedicine*, **84**, 153491 (2021).
- 21) Deshpande DA, Wang WCH, McIlmoyle EL, Robinett KS, Schilling RM, An SS, Sham JSK, Liggett SB. Bitter taste receptors on airway smooth muscle bronchodilate by a localized calcium flux and reverse obstruction. *Nat. Med.*, **16**, 1299–1304 (2010).
- 22) Tschumperlin DJ. Physical forces and airway remodeling in asthma. *N. Engl. J. Med.*, **364**, 2058–2059 (2011).
- 23) Gunst SJ. Contractile force of canine airway smooth muscle during cyclical length changes. *J. Appl. Physiol.*, **55**, 759–769 (1983).
- 24) Bossé Y. The strain on airway smooth muscle during a deep inspiration to total lung capacity. *J. Eng. Sci. Med. Diagn. Ther.*, **2**, 010802-1–010802-21 (2019).
- 25) Bates JHT, Rajendran V. Mitigation of airways responsiveness by deep inflation of the lung. *J. Appl. Physiol.*, **124**, 1447–1455 (2018).
- 26) Ito S. Stretch-activated calcium mobilization in airway smooth muscle and pathophysiology of asthma. *Current Opinion in Physiology*, **21**, 65–70 (2021).
- 27) Xiao B. Levering mechanically activated piezo channels for potential pharmacological intervention. *Annu. Rev. Pharmacol. Toxicol.*, **60**, 195–218 (2020).
- 28) Raudenska M, Kratochvilova M, Vicar T, Gumulec J, Balvan J, Polanska H, Pribyl J, Masarik M. Cisplatin enhances cell stiffness and decreases invasiveness rate in prostate cancer cells by actin accumulation. *Sci. Rep.*, **9**, 1660 (2019).
- 29) Syeda R, Xu J, Dubin AE, Coste B, Mathur J, Huynh T, Matzen J, Lao J, Tully DC, Engels IH, Petrassi HM, Schumacher AM, Montal M, Bandell M, Patapoutian A. Chemical activation of the mechanotransduction channel piezol. *eLife*, **4**, e07369 (2015).
- 30) Wang Y, Chi S, Guo H, Li G, Wang L, Zhao Q, Rao Y, Zu L, He W, Xiao B. A lever-like transduction pathway for long-distance chemical- and mechano-gating of the mechanosensitive piezol channel. *Nat. Commun.*, **9**, 1300 (2018).
- 31) Wang Y, Lu Y, Luo M, Shi X, Pan Y, Zeng H, Deng L. Evaluation of pharmacological relaxation effect of the natural product naringin on *in vitro* cultured airway smooth muscle cells and *in vivo* ovalbumin-induced asthma balb/c mice. *Biomed. Rep.*, **5**, 715–722 (2016).
- 32) Wang Y, Wang A, Zhang M, Zeng H, Lu Y, Liu L, Li J, Deng L. Artesunate attenuates airway resistance *in vivo* and relaxes airway smooth muscle cells *in vitro* *via* bitter taste receptor-dependent calcium signalling. *Exp. Physiol.*, **104**, 231–243 (2019).
- 33) Luo M, Ni K, Yu P, Jin Y, Liu L, Li J, Pan Y, Deng L. Sanguinarine decreases cell stiffness and traction force and inhibits the reactivity of airway smooth muscle cells in culture. *Mol. Cell. Biomech.*, **16**, 141–151 (2019).
- 34) Chen J, Rodriguez M, Miao J, Liao J, Jain PP, Zhao M, Zhao T, Babicheva A, Wang Z, Parmisano S, Powers R, Matti M, Paquin C, Soroureddin Z, Shyy JYJ, Thistlethwaite PA, Makino A, Wang J, Yuan JX-J. Mechanosensitive channel piezol is required for pulmonary artery smooth muscle cell proliferation. *Am. J. Physiol. Lung Cell. Mol. Physiol.*, **322**, L737–L760 (2022).
- 35) Wiggs BR, Hrousis CA, Drazen JM, Kamm RD. On the mechanism of mucosal folding in normal and asthmatic airways. *J. Appl. Physiol.*, **83**, 1814–1821 (1997).
- 36) Lauzon A-M, Martin JG. Airway hyperresponsiveness; smooth muscle as the principal actor. *F1000 Res.*, **5**, 306 (2016).
- 37) Ito S, Kume H, Naruse K, Kondo M, Takeda N, Iwata S, Hasegawa Y, Sokabe M. A novel Ca<sup>2+</sup> influx pathway activated by mechanical stretch in human airway smooth muscle cells. *Am. J. Respir. Cell Mol. Biol.*, **38**, 407–413 (2008).
- 38) Alper SL. Genetic diseases of Piezo1 and Piezo2 dysfunction. *Curr. Top. Membr.*, **79**, 97–134 (2017).
- 39) Tschumperlin DJ, Dai G, Maly IV, Kikuchi T, Laiho LH, McVittie AK, Haley KJ, Lilly CM, So PT, Lauffenburger DA, Kamm RD, Drazen JM. Mechanotransduction through growth-factor shedding into the extracellular space. *Nature*, **429**, 83–86 (2004).
- 40) Luo M, Yu P, Ni K, Jin Y, Liu L, Li J, Pan Y, Deng L. Sanguinarine rapidly relaxes rat airway smooth muscle cells dependent on Tas2r signaling. *Biol. Pharm. Bull.*, **43**, 1027–1034 (2020).
- 41) Bates JHT, Bullimore SR, Politi AZ, Sneyd J, Anafi RC, Lauzon AM. Transient oscillatory force-length behavior of activated airway smooth muscle. *Am. J. Physiol. Lung Cell. Mol. Physiol.*, **297**, L362–L372 (2009).
- 42) Jude JA, Wylam ME, Walseth TF, Kannan MS. Calcium signaling in airway smooth muscle. *Proc. Am. Thorac. Soc.*, **5**, 15–22 (2008).
- 43) Fay FS. Calcium sparks in vascular smooth muscle: Relaxation regulators. *Science*, **270**, 588–589 (1995).
- 44) Zhao QY, Peng YB, Luo XJ, *et al.* Distinct effects of Ca<sup>2+</sup> sparks on cerebral artery and airway smooth muscle cell tone in mice and humans. *Int. J. Biol. Sci.*, **13**, 1242–1253 (2017).
- 45) Bradley E, Large RJ, Bihun VV, Mullins ND, Hollywood MA, Sergeant GP, Thornbury KD. Inhibitory effects of openers of large-conductance Ca<sup>2+</sup>-activated K<sup>+</sup> channels on agonist-induced phasic contractions in rabbit and mouse bronchial smooth muscle. *Am. J. Physiol. Cell Physiol.*, **315**, C818–C829 (2018).
- 46) Zhang T, Luo X, Sai W, Yu M, Li W, Ma Y, Chen W, Zhai K, Qin G, Guo D, Zheng Y, Wang Y, Shen J, Ji G, Liu Q. Non-selective cation channels mediate chloroquine-induced relaxation in precontracted mouse airway smooth muscle. *PLOS ONE*, **9**, e101578 (2014).
- 47) Zhang C, Lifshitz LM, Uy KF, Ikebe M, Fogarty KE, ZhuGe R, ZhuGe R. The cellular and molecular basis of bitter tastant-induced bronchodilation. *PLOS Biol.*, **11**, e1001501 (2013).
- 48) Noble PB, Pascoe CD, Lan B, Ito S, Kistemaker LE, Tatler AL, Pera T, Brook BS, Gosens R, West AR. Airway smooth muscle in asthma: Linking contraction and mechanotransduction to disease pathogenesis and remodelling. *Pulm. Pharmacol. Ther.*, **29**, 96–107 (2014).
- 49) McHugh BJ, Buttery R, Lad Y, Banks S, Haslett C, Sethi T. Integrin activation by fam38a uses a novel mechanism of R-Ras targeting to the endoplasmic reticulum. *J. Cell Sci.*, **123**, 51–61 (2010).
- 50) Han Y, Liu C, Zhang D, Men H, Huo L, Geng Q, Wang S, Gao Y, Zhang W, Zhang Y, Jia Z. Mechanosensitive ion channel Piezol promotes prostate cancer development through the activation of the Akt/mTOR pathway and acceleration of cell cycle. *Int. J. Oncol.*, **55**, 629–644 (2019).
- 51) Chubinskiy-Nadezhdin VI, Vasileva VY, Vassilieva IO, Sudarikova AV, Morachevskaya EA, Negulyaev YA. Agonist-induced Piezol activation suppresses migration of transformed fibroblasts. *Biochem. Biophys. Res. Commun.*, **514**, 173–179 (2019).
- 52) McHugh BJ, Murdoch A, Haslett C, Sethi T. Loss of the integrin-activating transmembrane protein FAM38a (Piezo1) promotes a switch to a reduced integrin-dependent mode of cell migration. *PLOS ONE*, **7**, e40346 (2012).

- 53) Friedl P. Preshcification and plasticity: Shifting mechanisms of cell migration. *Curr. Opin. Cell Biol.*, **16**, 14–23 (2004).
- 54) Ross EC, ten Hoeve AL, Barragan A. Integrin-dependent migratory switches regulate the translocation of toxoplasma-infected dendritic cells across brain endothelial monolayers. *Cell. Mol. Life Sci.*, **78**, 5197–5212 (2021).
- 55) Mousawi F, Peng H, Li J, Ponnambalam S, Roger S, Zhao H, Yang X, Jiang LH. Chemical activation of the piezol channel drives mesenchymal stem cell migration *via* inducing ATP release and activation of P2 receptor purinergic signaling. *Stem Cells*, **38**, 410–421 (2020).
- 56) Li C, Rezanian S, Kammerer S, Sokolowski A, Devaney T, Gorischek A, Jahn S, Hackl H, Groschner K, Windpassinger C, Malle E, Bauernhofer T, Schreibmayer W. Piezol forms mechanosensitive ion channels in the human MCF-7 breast cancer cell line. *Sci. Rep.*, **5**, 8364 (2015).